Birefringence and tilt angle in the antiferroelectric, ferroelectric, and intermediate phases of chiral smectic liquid crystals

M. Škarabot,[1] Mojca Čepič,[2,1] B. Žekš,[3,1] R. Blinc,[4,1] G. Heppke,[5] A. V. Kityk,[1,*] and I. Muševič[4,1]
[1]*J. Stefan Institute, Jamova 39, 1111 Ljubljana, Slovenia*
[2]*Faculty of Education, Kardeljeva ploščad 16, 1000 Ljubljana, Slovenia*
[3]*Institute of Biophysics, Medical Faculty, Lipičeva 2, 1105 Ljubljana, Slovenia*
[4]*Faculty of Mathematics and Physics, University of Ljubljana, Jadranska 19, Ljubljana, Slovenia*
[5]*Iwan-N-Stranski-Institut, Technische Universität Berlin, Sekretariat ER 11, Str. des 17, Juni 135, D-10623 Berlin, Germany*
(Received 10 February 1998)

Using a high resolution optical polarimeter, we have measured the temperature dependence of the birefringence and optical rotation in chiral smectic liquid crystals that exhibit antiferroelectric, ferroelectric, and intermediate phases. The temperature dependence of the magnitude of the tilt angle was determined from the birefringence of 4-(1-methyl-heptyloxycarbonyl-phenyl) 4′-octylbiphenyl-4-carboxylate (MHPOBC) and of 4-(1-methylheptyloxycarbonyl-phenyl) 4′-octylcarbonyloxybiphenyl-4-carboxylate (MHPOCBC). Both substances exhibit a crossover of the order parameter exponent from the classical value of $\beta=0.5$ close to the transition to the tricritical value $\beta=0.25$ far away. This stresses the importance of the sixth order terms in the Landau free-energy expansion for ferroelectric and antiferroelectric liquid crystals. In addition, a discontinuous behavior in the magnitude of the tilt is observed when crossing the smectic-C_α^*–smectic-C^* or smectic-C^*–smectic-C_A^* transitions, whereas the smectic-A–smectic-C_α^* transition is continuous. The simultaneously determined optical rotation is used to elucidate the structures and the nature of phase transitions. The results are well explained within the framework of a discrete phenomenological model with nearest and next nearest neighbor interactions between the smectic layers. [S1063-651X(98)01607-9]

PACS number(s): 61.30.−v, 64.70.Md, 77.22.Gm

I. INTRODUCTION

The thermodynamic properties of chiral antiferroelectric (smectic-C_A^*), ferroelectric (smectic-C^*), and intermediate phases (smectic-C_α, smectic-C_γ^*) of chiral smectic liquid crystals have recently attracted a lot of attention. The reason for this is the extraordinary optical and electro-optical properties of these novel phases that have a great potential for application in flat panel displays. On the other hand, the rich variety of structures that are observed in these new smectic materials has initiated the development of a new theoretical approach for the description of phase transitions between these phases.

Experiments on freely suspended smectic films of thickness of several molecular smectic layers have clearly revealed the structure of the ferroelectric smectic-C^* and antiferroelectric smectic-C_A^* phases [1]. In the ferroelectric smectic-C^* phase, chiral molecules are spontaneously tilted at a tilt angle θ with respect to the layer normal. Due to chirality and polarity of the molecules, a macroscopic spontaneous polarization is observed in a direction normal to the tilt plane. The direction of the tilt and the spontaneous polarization slowly precess as we move along the layer normal. As a result, a helical structure is formed, with a helical period of the order of the wavelength of visible light. In the antiferroelectric smectic-C_A^* phase, the molecules are also tilted at a tilt angle θ with respect to the smectic layer normal, whereas the direction of the tilt alternates when we move from one smectic layer to the other. The direction of the in-plane spontaneous polarization $\vec{P}_i$, which is perpendicular to the plane of the local tilt, also reverses by nearly $\pm 180°$ on going from one smectic layer to another. Two neighboring layers thus form an antiferroelectric unit cell with two antiparallel electric dipoles and a very small value of the equilibrium electric polarization $\vec{P}_0(\vec{r})=\vec{P}_i+\vec{P}_{i+1} \approx 0$. Because of chirality, the directions of the spontaneous tilt and the in-plane polarization slowly precess around the layer normal as one moves along the direction perpendicular to the smectic plane. This causes a small deviation from the 180° alternation in the tilt and the polarization between two consecutive layers and the formation of a modulated, helicoidal superstructure. On the other hand, there is not yet any direct evidence of the molecular structure in the so-called ferrielectric smectic-C_γ^* and smectic-C_α phases. There are a number of dielectric [2], optical [3], and electro-optical [4] experiments that can help conjecture on what the symmetry of these phases might be, but none of these experiments can give a direct insight into the structure on the molecular level.

The thermodynamic properties and phase transitions between the antiferroelectric smectic-C_A^* phase and the related ferrielectric, ferroelectric, and paraelectric phases have been theoretically analyzed by Orihara and Ishibashi [5] and later by Žekš and Čepič [6]. This theoretical description is of a continuous nature and implies the introduction of two order parameters, i.e., the ferroelectric and the antiferroelectric order parameters $\vec{\xi}_f$ and $\vec{\xi}_a$, respectively [5]. In this sense, it is clear that this continuum theory can reproduce only four different structures: (i) the paraelectric smectic-A phase, where

*On leave from the Institute of Physical Optics, Dragomanova strasse 23, 290005 Lviv, Ukraine.

both equilibrium order parameters equal zero; (ii) the ferroelectric phase where the ferroelectric order parameter is nonzero, $\vec{\xi}_f \neq 0$; (iii) the antiferroelectric smectic-C_A^* phase where the antiferroelectric order parameter is nonzero, $\vec{\xi}_a \neq 0$; (iv) the ferrielectric smectic-C_γ^* phase, where both order parameters are nonzero, $\vec{\xi}_f \neq 0, \vec{\xi}_a \neq 0$.

The problem of the structure of the smectic-C_α phase has initiated the development of several discrete phenomenological models, for the description of the intermediate phases (i.e., smectic-C_α and smectic-C_γ) [7–10]. Among them, the ANNNI model of Yamashita [7] and the discrete model of Čepič and Žekš [8,9] seem to be most complete. In the ANNNI (anisotropic next-nearest-neighbor interaction) model of Yamashita, the molecules in the ith smectic layer are tilted at a constant (i.e., temperature independent) tilt angle, but the direction of the tilt of the molecules in the neighboring layers is constrained into the plane of the tilt of the ith layer. There are therefore two allowed directions of the molecular tilt in this model. By considering the interactions between neighboring layers up to next-nearest neighbors, Yamashita has found different phase sequences between the equilibrium structures. The constraint of keeping the directions of the molecular tilt in a single plane has been released in the theory of Čepič and Žekš [8,9]. Here, the tilt directions of the molecules in the neighboring layers are allowed to make arbitrary angles as one moves from one smectic layer to another.

The temperature dependence of the tilt angle in ferroelectric, intermediate, and antiferroelectric phases of MHPOBC has already been measured [11]. The present work has been initiated by the possibility of high-resolution measurements of the tilt angle in tilted chiral smectics via the measurements of the optical birefringence [12]. The tilt angle, which is a symmetry breaking variable in these phases, dominates the free-energy expansion. Precise measurements of this quantity can therefore give valuable information on the relevance of various terms in the free-energy expansion and can eventually rule out certain models. The tilt angle was measured indirectly by measuring the birefringence of a tilted, helical structure, without applying any disturbing electric fields. Recently, it was shown for the ferroelectric liquid crystal CE-8 [12], that the measurements of birefringence of helical tilted phases can give very accurate values of the tilt angle. An agreement of better than 5% between the tilt angle, as determined from x-ray switching in electric field and birefringence data, has been observed for CE-8.

The theoretical part of this work briefly describes the discrete model and gives the set of relations between the parameters of the free-energy expansion. The experimental arrangement and procedures are described in the third section. Section IV presents the simultaneous measurements of birefringence and optical rotation, together with the calculation of the tilt angle and a discussion of the experimental results.

II. THEORY

The free energy of a tilted smectic liquid crystal is within the discrete phenomenological model [13] given by

$$G=\sum_j \tfrac{1}{2}a_0\xi_j^2+\tfrac{1}{4}b_0\xi_j^4+\tfrac{1}{6}c_0\xi_j^6+\tfrac{1}{2}A_1(\vec{\xi}_j\cdot\vec{\xi}_{j+1}) +\tfrac{1}{8}A_2(\vec{\xi}_j\cdot\vec{\xi}_{j+2})+\tfrac{1}{4}B_1(\vec{\xi}_j\cdot\vec{\xi}_{j+1})^2+\tfrac{1}{2}f(\vec{\xi}_j\times\vec{\xi}_{j+1})_z. \quad (1)$$

Here, $\vec{\xi}_j$ is a two-dimensional tilt order parameter that describes the magnitude and the direction of the molecular tilt of the jth smectic layer. The normal to the layers is assumed to be along the z direction. The coefficient of the harmonic term is linearly temperature dependent, $a_0=a(T-T_0)$ whereas other coefficients are constant. T_0 is here the phase transition temperature into a tilted phase for a system of smectic layers without interlayer interactions. Because the transition to the tilted phase can be either continuous or of the first order, both fourth- and sixth-order terms have to be considered. The coefficient A_1 determines the tilt orientation of the order parameters in neighboring layers and, depending on its sign, favors either ferroelectric or antiferroelectric order. Similarly, the coefficient A_2 determines the tilt orientation in next-nearest-neighboring layers. The coefficient B_1 corresponds to the interactions between quadrupolarly ordered transverse molecular dipoles in two neighboring layers and is always positive. This means that it prefers perpendicular tilt directions in neighboring layers. The coefficient f is of chiral origin and is expected to be small with respect to the rest of the coefficients. The summation is taken over N smectic layers in a system.

X-ray experiments have shown that the magnitude of the tilt is spatially homogeneous in the antiferroelectric and intermediate phases, so that the order parameter can be written as

$$\vec{\xi}_j=\theta(\cos\ \varphi_j \sin\ \varphi_j). \quad (2)$$

Here, θ is the magnitude of the tilt and φ_j is the corresponding phase angle of the tilt in the jth layer.

The coefficients A_1, A_2, and B_1 give the magnitude of interlayer interactions, that are composed of steric, Van der Waals, and electrostatic contributions [9]. Steric interactions act only between nearest-neighboring layers and originate in an incomplete smectic ordering and in consequent interpenetration of molecules. Van der Waals and electrostatic interactions vanish between two positionally uncorrelated liquid layers and their range is therefore limited by the range of interlayer positional correlations. They are expected to decrease by lowering the temperature (i.e., by increasing the tilt angle), because of the increasing smectic order and decreasing interpenetration, that facilitates the lateral motion of molecules. The coefficients A_1, A_2, and B_1 are therefore complicated functions of θ that include the effect of θ on the interlayer positional correlations and on the intermolecular distances that effect the intermolecular and Van der Waals interactions. For small tilt angles, these functions can be represented by expansion as

$$A_1=a_1+a_1'\theta^2+a_1''\theta^4, \quad (3a)$$

$$A_2=a_2+a_2'\theta^2+a_2''\theta^4, \quad (3b)$$

$$B_1=b_1+b_1'\theta^2, \quad (3c)$$

and the corresponding free energy is

$$G=\sum_j \tfrac{1}{2}a_0\theta^2+\tfrac{1}{4}b_0\theta^4+\tfrac{1}{6}c_0\theta^6+\tfrac{1}{2}(a_1+a_1'\theta^2+a_1''\theta^4)\theta^2\times\cos(\varphi_{j+1}-\varphi_j)+\tfrac{1}{8}(a_2+a_2'\theta^2+a_2''\theta^4)\theta^2\times\cos(\varphi_{j+2}-\varphi_j)+\tfrac{1}{4}(b_1+b_1'\theta^2)\theta^2\cos^2(\varphi_{j+1}-\varphi_j)+\tfrac{1}{2}f\theta^2\sin(\varphi_{j+1}-\varphi_j). \quad (4)$$

Stable solutions for θ and φ_j are obtained by minimizing this free energy with respect to θ and all phase angles φ_j, simultaneously. It turns out that only two classes of solutions are stable, depending on the sign of the coefficient A_2.

For a positive A_2, $A_2>0$, there are three characteristic stable solutions, that correspond to three different structures, as shown in Figs. 1(a)–1(c). In these three solutions, the difference between the phase angles α in neighboring layers is constant. The phase angle therefore increases monotonically, as we move along the smectic layer normal and the solutions differ only in the *magnitude* of this phase difference. The first solution, shown in Fig. 1(a), obviously corresponds to the ferroelectric smectic-C^* phase. Here, the phase angle between the molecules in neighboring layers is very small and originates from the chirality of the molecules. The second solution is shown in Fig. 1(b) and corresponds to the antiferroelectric smectic-C_A^* phase. Here, the phase between the directions of the tilt in neighboring layers increases nearly by π, as we move along the layer normal. The small deviation from the antiparallel ordering is again caused by the chiral term in the free energy [Eq. (1)]. The third solution is shown in Fig. 1(c) and corresponds to a novel structure that we identify as the smectic-C_α phase. Here, the phase angle between the directors in neighboring layers has a finite value between zero and π. The smectic-C_α phase is here in fact a short pitch helicoidal structure, which is structurally equivalent to the well-known chiral ferroelectric smectic-C^* phase. However, the origin of this short, nanometer-sized helix is completely different from the origin of the helix in the ferroelectric smectic-C^* phase. Whereas the helix in chiral ferroelectric smectic-C^* phase originates from the chirality of the molecules, it arises in the smectic-C_α phase due to the competition between the interactions between the nearest neighboring and the next nearest neighboring layers. In the smectic-C_α phase, the chirality removes the degeneracy between the left handed structure and the right handed one, that exists for achiral systems. Because of the short pitch, this smectic-C_α phase is expected to show a very small optical rotation and is therefore expected to behave optically as the smectic-A phase. Also, relatively large external electric fields are needed to unwind the helicoidal structure, which is consistent with experimental observations. All these three phases have the same symmetry and can therefore transform continuously one into another without any anomaly. One can therefore experimentally identify the smectic-C_α phase as a distinct phase, only when the transition between the smectic-C_α phase and the smectic-C^* phase is of first order.

For a negative A_2, $A_2<0$, there is only one stable solution, shown in Fig. 1(d), which is different from those already mentioned. Here, the phase angle behaves nonmonotonically, as we move along the normal to the smectic layers. First, it increases for a finite value of α, as we move to the nearest neighbor, but when we reach the next-nearest neighbor, the phase angle nearly ''flips back'' to the original value. The structure can also be considered as a double-twist structure, formed by two identical ferroelectric helices, gearing into each other. Here, the helices are rotated with respect to each other at a finite phase angle $0<\alpha<\pi$. It is conjectured that this structure corresponds to the ferrielectric smectic-C_γ^* phase.

For a given material, the signs and the ratios of the coefficients in the free-energy expansion Eq. (4) are not arbitrary. It turns out that they are determined by (i) the sequence of

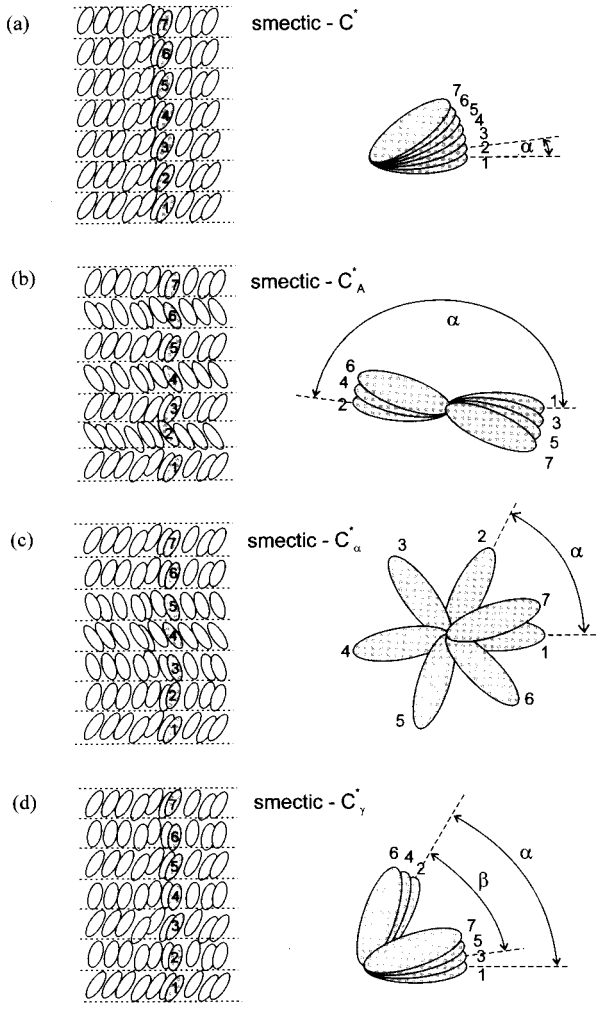

FIG. 1. The equilibrium structures, as obtained within the discrete layer model with interlayer interactions up to the next nearest neighbor: (a) The ferroelectric smectic-C^* phase is characterized by a small value of α, giving rise to a monotonously growing phase angle, as we move along the layer normal. (b) The antiferroelectric smectic-C_A^* phase is characterized by a doubled unit cell, composed, say, of molecules 1 and 2, as indicated. In this phase α is close to π. (c) The smectic-C_α^* phase is characterized by the ''rapid winding'' of the phase angle, as we move along the layer normal of these materials. This phase is in fact a short-pitch ferroelectric phase with $0<\alpha<\pi$. (d) The ferrielectric smectic-C_γ^* phase is characterized by an alternate behavior of the phase angle. The phase first increases for α, as we move to the next layer and then ''flips back'' for an angle β as we move to the third layer. Note that the structures of the smectic-C_α^* and smectic-C_γ^* phase have not yet been experimentally verified.

phases, (ii) the phase transition temperatures, and (iii) the values of the tilt angle at the phase transition temperatures between different intermediate phases. For example, the antiferroelectric liquid crystal MHPOBC has the following sequence of phases: smectic-A–smectic-C_α–smectic-C^*–smectic-C^*_γ–smectic-C^*_A. This phase sequence implies the following signs and relations between the coefficients: $a_1<0$, $a_2>0$, $a_1'>0$, $a_2'<0$, and $|a_1|<|a_2|$. Further, at each phase transition temperature we get a system of two algebraic equations for the coefficients. This richness of phase sequences therefore allows us to (i) test the applicability of this theory on real substances, and (ii) determine the values of free-energy expansion coefficients. It is easy to understand that in materials with less intermediate phases, the number of coefficients that can be determined is substantially smaller. If we consider, for example, a material that has only the ferroelectric smectic-C^* phase, we can determine from the measurements of the temperature dependence of the tilt angle only the expansion coefficients of the second, fourth, and sixth order power terms in the tilt. One can see from the form of the free-energy expansion Eq. (4), that this determines only the sum of certain coefficients, whereas the values of individual coefficients cannot be resolved.

Measurements of the temperature dependence of the tilt angle in materials that show intermediate phases are therefore a good test for the theory. In tilted smectic phases, the tilt angle can be measured in several different ways: (i) using x-ray diffraction to determine the change of the interlayer distance due to the tilting of the molecules, (ii) using the electrooptic response of a tilted smectic in thin cells to a large electric field, and (iii) measuring the birefringence in tilted, helicoidally modulated smectic phases. The latter method is advantageous with respect to (ii), because the structure is not disturbed. We have also shown that this method gives identical results to x-ray diffraction and electric switching in CE8.

Briefly, the optical properties of a tilted, helicoidally modulated smectic liquid crystal can be in the first order approximated by the optical properties of an uniaxial smectic-A phase [12,14]. The corresponding dielectric tensor is the space-averaged dielectric tensor of the real structure in question. For example, the space-averaged dielectric tensor of the chiral ferroelectric smectic-C^* is equal to the space averaged dielectric tensor of the chiral antiferroelectric smectic-C^*_A phase and is an uniaxial tensor

$$\langle \underline{\varepsilon} \rangle = \begin{vmatrix} \langle \varepsilon \rangle_{xx} & 0 & 0 \\ 0 & \langle \varepsilon \rangle_{yy} & 0 \\ 0 & 0 & \langle \varepsilon \rangle_{zz} \end{vmatrix} \tag{5}$$

with

$$\langle \varepsilon \rangle_{xx} = \tfrac{1}{2}[(\varepsilon_1+\varepsilon_2)+(\varepsilon_3-\varepsilon_2)\sin^2\theta], \tag{6a}$$

$$\langle \varepsilon \rangle_{yy} = \tfrac{1}{2}[(\varepsilon_1+\varepsilon_2)+(\varepsilon_3-\varepsilon_2)\sin^2\theta], \tag{6b}$$

$$\langle \varepsilon \rangle_{zz} = \varepsilon_3-(\varepsilon_3-\varepsilon_1)\sin^2\theta. \tag{6c}$$

Here, ε_1 and ε_2 are the components of the dielectric tensor of the paraelectric smectic-A phase in two directions perpendicular to the long molecular axis and ε_3 is the dielectric constant, measured along the long molecular axis. The corresponding average refractive indices are tilt dependent. In the limit of small tilt angles, the birefringence of smectic-C^* and smectic-C^*_A phase is

$$\overline{n_e}-\overline{n_o} \cong (n_e-n_o)-C\,\sin^2\theta. \tag{7}$$

Here, (n_e-n_o) is the background birefringence that depends on the nematic order parameter and C is a constant. The birefringence of the tilted helicoidally modulated smectic phases is therefore always smaller than the birefringence of the smectic-A phase and this difference is proportional to the square of the order parameter. This effect can be easily understood: when the molecules tilt in the chiral phases, the ''in-plane'' component of the dielectric tensor increases, whereas the component of the dielectric tensor along the layer normal decreases. This gives a slight decrease of the extraordinary index of refraction and a slight increase of the ordinary index of refraction due to molecular tilt. As a result, the birefringence decreases in tilted, helicoidally modulated phases, as indeed observed in the experiments [12].

It can be seen from Eq. (7) that it is possible to determine the temperature dependence of the tilt angle in an unperturbed helicoidally modulated smectic phase via the temperature dependence of the birefringence. These measurements can be performed with great experimental accuracy and therefore high-resolution tilt data can easily be obtained. However, one should keep in mind that this is only a first-order approximation to the optical properties of helicoidal tilted smectic phases, which breaks down in the cases of degeneration of the optical eigenmodes. This corresponds to the propagation of light along the helix or at a Bragg angle, and should be avoided in the experiment.

III. EXPERIMENT

The setup for the high-resolution measurements of the birefringence is shown in Fig. 2. We have also measured simultaneously the optical rotation of linearly polarized light, propagating along the helical axis. We have used a high-resolution optical polarization method for the accurate determination of the birefringence and optical rotation. The setup is based on an optical photoelastic modulator (PEM-90, Hinds Instrum.) and uses a dual lock-in detection to minimize the effects of the uncontrolled light-intensity fluctuations. The orientation of the axes of anisotropy for each optical element are indicated with respect to the initial polarization of the laser beam. The intensity of the modulated light was detected by a photodiode and two lock-in amplifiers, which simultaneously determined the amplitudes of the first and second harmonics, respectively.

The birefringence of the sample was measured for light propagating at an angle β with respect to the optical axis, whereas the optical rotation of the sample was measured for light propagating along the normal to the smectic layers. Two He-Ne lasers with the wavelength $\lambda_o = 0.6328\ \mu$m were used for birefringence and optical rotation measurements. Both lasers were slightly focused to a single spot on the sample with the diameter of $\approx 10\ \mu$m by carefully adjusting the positions of the laser beams. The values of the birefringent retardation B and the optical rotation angle Ψ can be

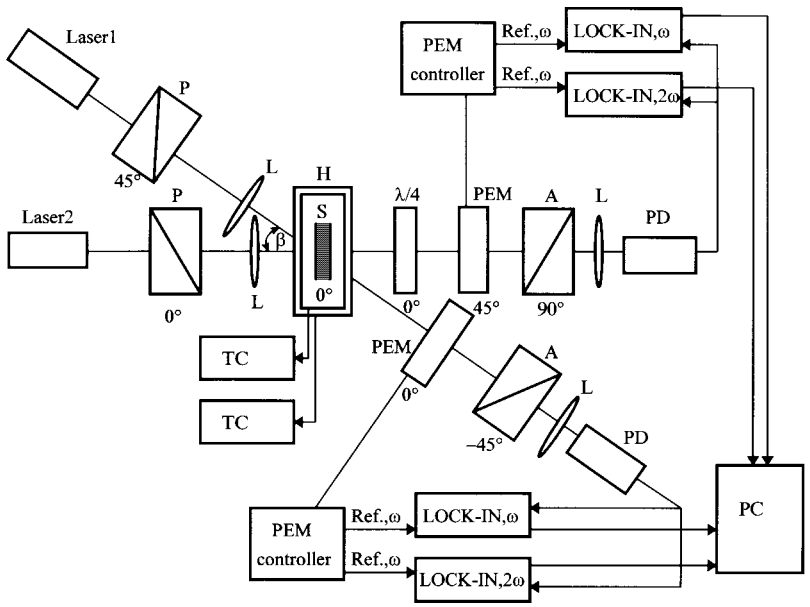

FIG. 2. The experimental setup for the simultaneous measurements of the birefringence and optical rotation. *P*, polarizer; *A*, analyzer; *L*, lens; *PD*, photodiode; PEM, photoelastic modulator; TC, temperature controller; *S*, sample; *H*, double stage heater with ± 2 mK stability.

determined from the general expression for the light intensity at the detector, first derived by Kemp [15]. Here, the retardation $B=2\pi/\lambda_o[n_e(\beta)-n_o]d$ is measured at an angle β with respect to the optical axis, and d is the length of the optical path through the sample, which is determined by the sample thickness and β. For the setup in Fig. 2, the retardation of the sample is

$$B=\arctan\left(\frac{U_{1\Omega}}{U_{2\Omega}}\frac{J_2(A_0)}{J_1(A_0)}\right), \tag{8}$$

whereas the optical rotation is

$$\Psi=\tfrac{1}{2}\arctan\left(\frac{U_{1\Omega}}{U_{2\Omega}}\frac{J_2(A_0)}{J_1(A_0)}\right). \tag{9}$$

Here $U_{1\Omega}$ and $U_{2\Omega}$ are the amplitudes of the first and second harmonic, respectively. $J_1(A_0)$ and $J_2(A_0)$ are the values of Bessel functions at a constant amplitude of retardation A_0, which is defined by the photoelastic modulator. In our studies, we used a modulation frequency $\Omega=50$ kHz and the retardation amplitude $A_0=0.383\lambda$. The relative accuracy for both types of measurements was 0.01°. The absolute value of the birefringence was determined in the smectic-*A* phase. This was done by changing the angle β from zero to the value used in the temperature scans and monitoring the number of fringes, detected by the lock-in amplifiers. The thickness of the sample was determined with a spectrophotometer.

Liquid crystals were aligned homeotropically in DMOAP silane-treated cells of thickness 120 μm. A good optical quality of the samples was achieved in the smectic-C^*_α, smectic-C^* and smectic-C^*_A phases of 4-(1-methylheptyloxycarbonyl-phenyl) 4′-octylbiphenyl-4-carboxylate (MHPOBC), and 4-(1-methylheptyloxycarbonyl-phenyl) 4′-octylcarbonyloxybiphenyl-4-carboxylate (MHPOCBC). On the contrary, a large number of defects was always observed in the smectic-C^*_γ phase of MHPOBC, which is consistent with other observations [11]. This phase could not be well aligned even in much thinner, 20 μm homeotropic cells. The samples were placed in a double stage temperature controlled oven with a temperature control better than 4 mK. The temperature dependence of the retardation and optical rotation were measured by slowly and continuously decreasing the temperature of the sample at a rate of 20 mK per minute. A typical experiment run lasted for 12 h.

IV. RESULTS AND DISCUSSION

The temperature dependence of the birefringence and optical rotation power (ORP) in the antiferroelectric liquid crystal (R)-MHPOBC is shown in Fig. 3 for a very large temperature range. Figures 4(a) and 4(b) show the same data for the narrow region of intermediate phases. The following features can be observed in these data, which are also characteristic for other materials, showing antiferroelectric and intermediate phases: (i) In the smectic-*A* phase, the birefringence increases monotonically with decreasing temperature, which is due to a gradual increase of the nematic order parameter with decreasing temperature. (ii) Several degrees above the phase transition into the tilted phase, a significant deviation from this monotonous behavior is observed. The birefringence even starts to decrease gradually, as we approach the phase transition into the tilted phase. We conjecture that this is due to large fluctuations of the tilt angle in this pretransitional regime, which tend to decrease the birefringence. Similar fluctuation effects were observed in heat capacity studies of these materials, and long ago in the first studies of the birefringence in the vicinity of the smectic-*A*–smectic-*C* transition [16]. (iii) A strong and monotonic decrease of birefringence is observed in the tilted phase, as expected from the theory. (iv) Discontinuous jumps of the birefringence are observed at the smectic-C^*_α to smectic-C^* phase and between the smectic-C^* and smectic-C^*_A phase. These jumps of the birefringence are new and

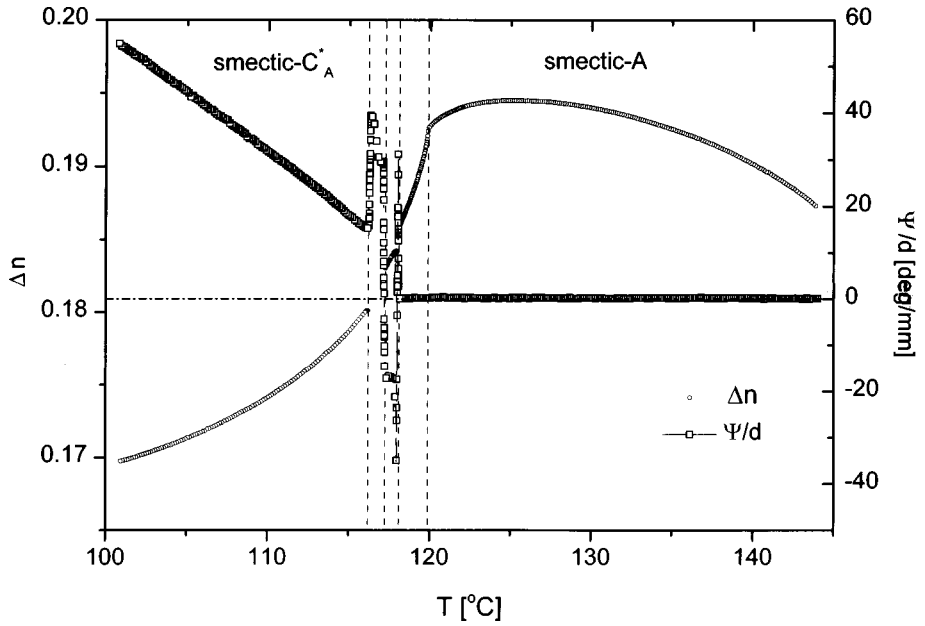

FIG. 3. The temperature dependence of the birefringence and optical rotation per unit length in (R)-MHPOBC.

surprising and are shown in Fig. 4(a). (v) The birefringence could not be determined in the smectic-C^*_γ phase due to the presence of defects. In all experiments, the phase transition temperatures could be determined with an accuracy of 10 mK by monitoring the discontinuities in the birefringence and simultaneously measured ORP data.

The tilt angle was calculated from these data by the following procedure: A large temperature interval was chosen in the smectic-*A* phase, starting at the isotropic transition and ending several degrees above the transition into the tilted phase. The temperature dependence of the birefringence in this temperature region was fitted to the power law, in order to describe the gradual increase of the birefringence due to the increase of the nematic order parameter. This curve was then used as a background correction in the tilted phases. This procedure is analogous to the background correction in the heat-capacity studies. We have made sure that the length of the temperature interval, chosen in the smectic-*A* phase, does not significantly influence the values of the tilt angle thus determined. This is indeed the case when the temperature region of the smectic-*A* phase is wide enough, as the background-correction curve is already quite smooth and saturated in the region far away from the isotropic phase.

The temperature dependence of the tilt angle in different phases of (R)-MHPOBC, as determined from the birefringence data, is shown in Fig. 5. The inset to this figure shows a log-log plot of the data and reveals an important fact. There are obviously two regimes in the temperature dependence of the tilt: Close to the smectic-*A* phase, the exponent for the tilt angle is $\beta \approx 0.5$, as expected from the Landau free-energy expansion including fourth order term. However, several degrees below the smectic-*A* phase, the tilt exponent changes to $\beta \approx 0.25$, which is characteristic of a Landau tricritical behavior. It is well known since the work of Huang and Viner [17] that it is then necessary to include sixth order terms in the free-energy expansion, as we did in our theoretical analysis. The crossover temperature is several degrees below the smectic-*A* phase, i.e., in the region where the transitions to the smectic-C^*, smectic-C^*_γ, and smectic-C^*_A phases are observed. It is then clear that any theory, which tends to describe these phase transitions, should include tilt expansion up to the sixth order, because these are the dominant terms in the free-energy expansion.

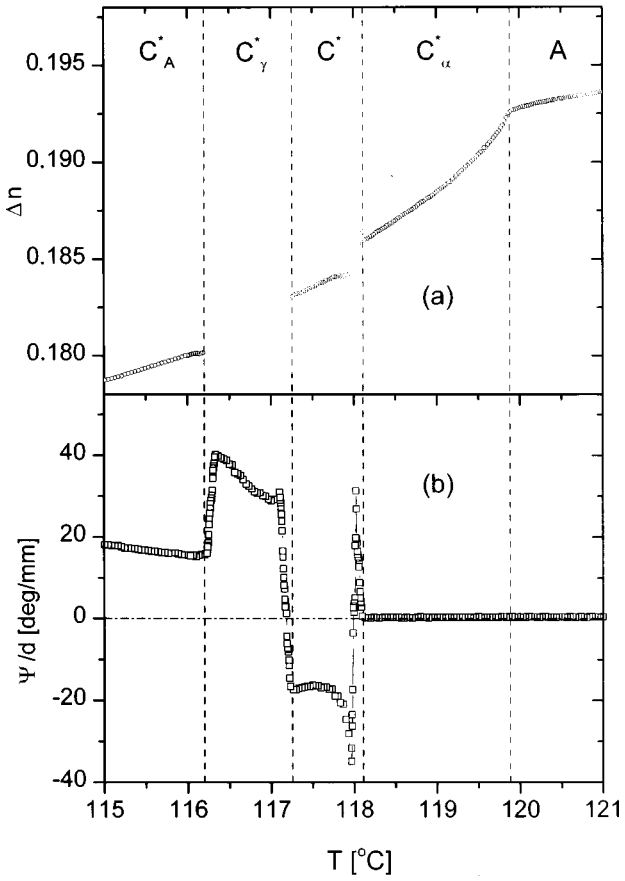

FIG. 4. (a) The temperature dependence of the birefringence in the intermediate phases of (R)-MHPOBC. (b) The temperature dependence of the optical rotation per unit length in (R)-MHPOBC.

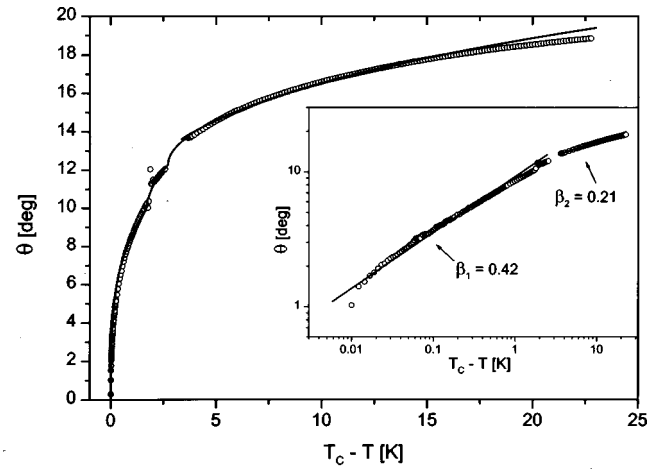

FIG. 5. The temperature dependence of the tilt angle in (R)-MHPOBC. The solid line is the best fit to the discrete model with the parameters given in the text. The inset shows the same data in a log-log scale to present the crossover of the power-law behavior of the tilt angle. Solid lines in the inset are the best power-law fits for the temperature interval 0.5 K below T_c and for the temperature interval 4 K$<T_c-T<$15 K, respectively.

The experimental data were fitted to the theory using the following procedure. The free energy is

$$G=\tfrac{1}{2}A(\alpha,T)\,\theta^2+\tfrac{1}{4}B(\alpha)\,\theta^4+\tfrac{1}{6}C(\alpha)\,\theta^6, \tag{10}$$

where the expansion coefficients $A(\alpha,T)$, $B(\alpha)$, and $C(\alpha)$ depend on the type of structure and we have neglected the chirality. In the smectic- C^*, smectic-C_A^*, and smectic-C_α^* phase they have the form

$$A(\alpha,T)=a(T-T_0)+a_1\cos\,\alpha+\tfrac{1}{4}a_2\cos 2\alpha, \tag{11a}$$

$$B(\alpha)=b_0+b_1\cos^2\alpha+2a_1'\cos\,\alpha+\tfrac{1}{2}\,a_2'\cos 2\alpha, \tag{11b}$$

$$C(\alpha)=c_0+\tfrac{3}{2}b_1'\cos^2\alpha+3a_1''\cos\,\alpha+\tfrac{3}{4}a_2''\cos 2\alpha. \tag{11c}$$

In the smectic-C_γ^* phase, $\cos 2\alpha$ is replaced by 1, because the phase difference between order parameters in next-nearest layers is zero for a nonchiral material. After minimizing the free energy with respect to θ, we can express the temperature difference as a function of the tilt:

$$(T_c-T)=\frac{A(\alpha,T_c)}{a}+T_0+\frac{B(\alpha)}{a}\,\theta^2+\frac{C(\alpha)}{a}\,\theta^4. \tag{12}$$

Here, T_c is the transition temperature to the tilted phase and T_0 is the temperature, where the tilted phase would appear in the absence of interlayer interactions.

The phase difference between the tilt directions in nearest layers defines the structure of the phase and is zero in the ferroelectric smectic-C^* phase, and equals π in the antiferroelectric smectic-C_A^* phase. In the smectic-C_α^*, minimization of the Eq. (4) gives the following approximation for the tilt angle dependence of the phase difference α:

$$\cos\,\alpha=-\frac{a_1+a_1'\theta^2+a_1''\theta^4}{a_2+(a_2'+b_1)\,\theta^2+(a_2''+b_1')\,\theta^4}. \tag{13}$$

In the smectic-C_γ^* phase, it has a slightly different tilt angle dependence

$$\cos\,\alpha=-\frac{a_1+a_1'\theta^2+a_1''\theta^4}{b_1\theta^2+b_1'\theta^4}. \tag{14}$$

First, we fit the experimental data in the temperature region of the ferroelectric phase, where $\cos\alpha\cong 1$, and in the temperature region of the antiferroelectric phase, where $\cos\alpha\cong -1$. By taking into account that the tilt equals zero at T_c and $\cos\alpha=-a_1/a_2$ at the transition temperature, we can obtain the values of parameters a_1, a_2, a_1', a_1'' and three algebraic relations for the rest of parameters. The values of b_1 and b_1' are calculated from the relation [Eq. (14)] for the values of the tilt angle at the transition from the smectic-C_γ^* phase to the ferroelectric phase, where $\cos\alpha=1$, and at the transition from the smectic-C_γ^* phase to the antiferroelectric phase, where $\cos\alpha=-1$. In a similar way we obtain the relation between a_2' and a_2'' from the value of the tilt angle at the transition from the smectic-C_α^* to the ferroelectric smectic-C^* phase. We are therefore left with a single free parameter a_2'', which is used to fit the temperature dependence of the tilt angle in the smectic-C_α^* phase.

The experimental data for MHPOBC, which shows a rich variety of phase transitions, can be very well fitted to the predictions of this theory. The parameters of the fit for MHPOBC together with their estimated accuracy are $a_1/a_2=-1.1(1\pm0.2)$, $a_1'/a=30.6(1\pm0.05)$, $a_1''/a=-192(1\pm0.03)$, $a_2/a=2.5$, $a_2'/a=-77.8(1\pm0.2)$, $a_2''/a=400(1\pm0.2)$, $b_1/a=2.4(1\pm0.2)$, $b_1'/a=-20.5(1\pm0.2)$, $b_0/a=-3.5(1\pm0.2)$, and $c_0/a=1400(1\pm0.2)$. We have also checked that this set of parameters corresponds to the global minimum of the free energy. The accuracy of the parameters was estimated by monitoring the behavior of the least-square fit with respect to small variations of the fitting parameters. It is important to note that the relative accuracy of the parameters is rather good, which is due to the high resolution of the experimental data. One should mention here that the signs of the coefficients a_1 and a_1' determined from the temperature dependencies of the tilt angle in the ferroelectric and in the antiferroelectric phase are in agreement with the relations between the coefficients required to obtain the experimentally observed phase sequence. Furthermore, it is nearly impossible to fit the experimental data with a set of parameters with different signs. This can be considered a clear indication of the internal consistency of the model.

The model parameters also allow for the analysis of the Landau behavior. It turns out that the fourth order coefficient $B(\alpha)$ is positive at the smectic-A–smectic-C_α^* transition, which is therefore of second order. However, structural changes from the smectic-C_α^* to the smectic-C^* phase result in a change of sign of this $B(\alpha)$ term, which becomes negative already in the ferroelectric smectic-C^* phase. This means that in a similar material without the smectic-C_α^* phase, the smectic-A–smectic-C^* would be of first order. Furthermore, the smallness of the $B(\alpha)$ term implies nearly tricritical behavior of the smectic-A–smectic-C_α^* transition in MHPOBC.

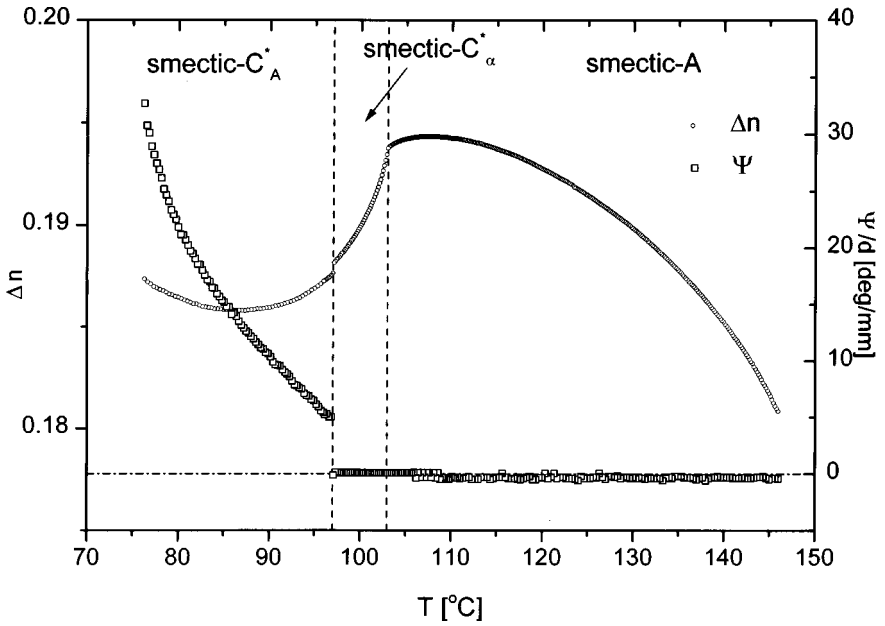

FIG. 6. The temperature dependence of the birefringence and optical rotation per unit length in (S)-MHPOCBC for a large temperature interval. Note the discontinuity of the birefringence at the smectic-C_α^*–smectic-C_A^* transition.

The temperature dependence of the birefringence and optical rotation in MHPOCBC are shown for a large temperature interval in Fig. 6 and for a narrow interval in Fig. 7. This compound has only the smectic-C_α^* and the antiferroelectric smectic-C_A^* phase. Again, one can clearly see the discontinuity of the tilt angle at the smectic-C_α^*–smectic-C_A^* phase transition, which is also accompanied by a discontinuous appearance of a finite ORP. We have observed that the tilt angle of MHPOCBC (Fig. 8) as calculated from the birefringence data, saturates in the antiferroelectric phase 20 K below T_c. A similar behavior was observed in EHPOCBC and tolane antiferroelectric liquid crystalline compounds. Because of the saturation behavior of the tilt far below T_c in the antiferroelectric phase the Landau theory cannot be used here. We therefore abandon fitting of b_1 and b_1', since both parameters have in both stable phases the same effect as a_2' and a_2'' and we also limit the fitting range to the smectic-C_α^* phase. The values of the parameters that give the best fit for the temperature dependence of the tilt in the smectic-C_α^* phase of MHPOCBC are $a_1/a \approx 1.1$, $a_1'/a \approx -38$, $a_1''/a \approx 110$, $a_2/a \approx 2.75$, $a_2'/a \approx -82$, $a_2''/a \approx -90$, $b_0/a \approx 2.2$, and $c_0/a \approx 4450$. These parameters are of the same order of magnitude as the parameters determined for MHPOBC. Here, both higher order parameters in nearest and next-nearest interactions were neglected, since they did not affect the shape of the fitting curve significantly.

Simultaneous measurements of the birefringence and optical rotation can give a deeper insight into the structure of stable phases. The temperature dependence of the optical rotation per unit thickness of (R)-MHPOBC was determined simultaneously with the birefringence of the sample and is shown in Figs. 3 and 4(b).

In the smectic-C_α^* phase, which is clearly a tilted phase, we could not detect any rotation of polarization. The optical rotatory power of this phase, if any, is smaller than 8×10^{-2} deg/min. This could be a result of a very short helical period p_0 of the smectic-C_α^* phase and supports the model of Čepič and Žekš [8,9]. Following de Vries theory, the optical rotation of the ferroelectric smectic-C^* phase is [18]

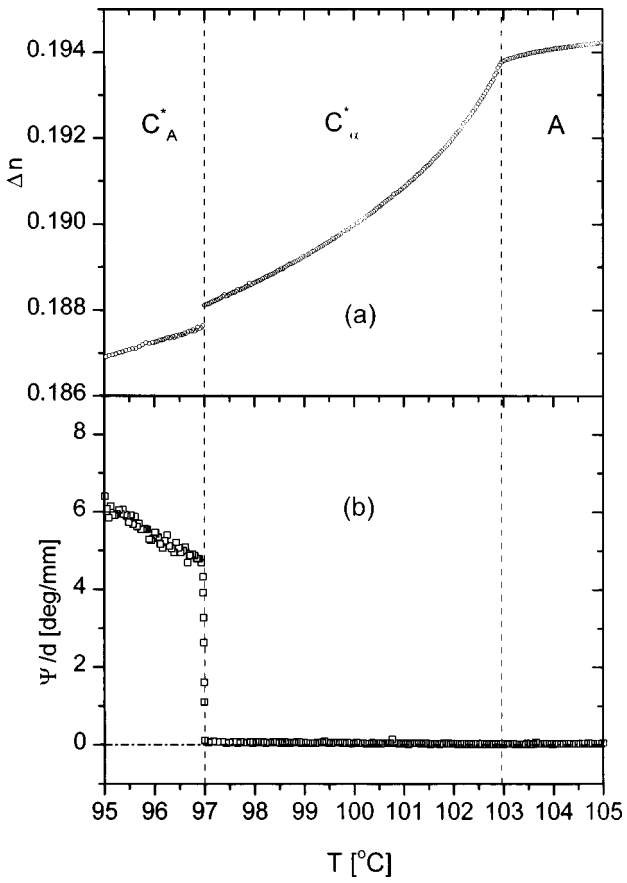

FIG. 7. The temperature dependence of (a) the birefringence and (b) the optical rotation per unit length in MHPOCBC in the vicinity of phase transitions into the smectic-C_α^* phase.

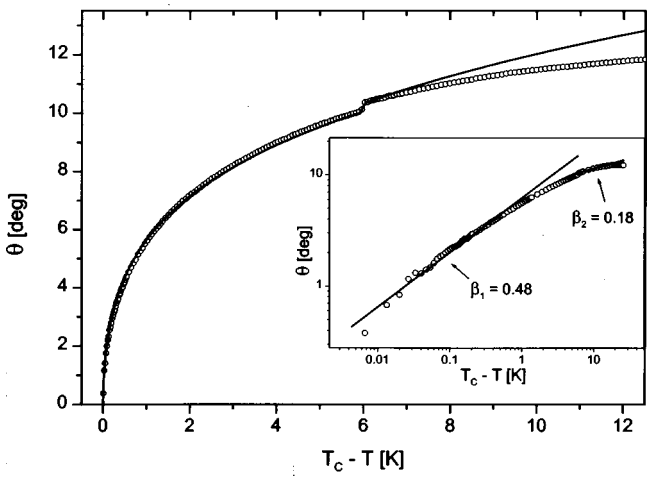

FIG. 8. The temperature dependence of the tilt angle in MHPOCBC, as determined from the birefringence. The solid line is the best fit to the discrete model with parameters given in the text. The inset shows the same data in a log-log scale to present the crossover of the power-law behavior of the tilt angle. Solid lines in the inset are the best power-law fits for the temperature interval 0.5 K below T_c and for the temperature interval $6\,\mathrm{K}<T_c-T<15\,\mathrm{K}$, respectively.

$$\rho=\frac{\Psi}{d}\approx p_0\vartheta^4. \tag{15}$$

A short calculation shows that for the tilt angle of ≈ 7 deg and the lower experimental detection limit of 8×10^{-2} deg/mm for the ORP, the helical period of the smectic-C^*_α phase in MHPOBC should be smaller than 150 nm.

The ORP is first detected in the ferroelectric smectic-C^* phase, as can be seen in Fig. 4(b). Here, one can clearly observe the characteristic anomaly of the ORP, which is due to the vicinity of the Bragg peak. Because the period of the helix $p(T)$ is temperature dependent, there will be an anomaly in the ORP, when the wavelength of light in the medium is equal to one-half of the helical period, i.e., $\lambda_0/(\varepsilon_\parallel+\varepsilon_\perp)=p/2$. The ORP then stabilizes at a negative value in the ferroelectric phase, increases to zero at a temperature slightly below the smectic-C^*–smectic-C^*_γ transition, and further increases in the ferrielectric phase. This change of the sign of the ORP within the smectic-C^*_γ phase has indeed been predicted theoretically [19] and is a result of the change of handedness of the smectic-C^*_γ structure. The change of sign is accompanied by (i) the divergence of the helical pitch, and, (ii) by a sharply decreasing birefringence of the unit cell when the angle between the molecular directors in the neighboring layers approaches 90°. It seems that this scenario could lead to the characteristic crossover behavior of the ORP in the smectic-C^*_γ phase, but detailed calculations of the ORP in the intermediate phases is clearly needed. At the phase transition into the antiferroelectric phase, the ORP first decreases slightly and then grows monotonically with decreasing temperature. One can clearly see a nearly linear increase of the ORP over a wide temperature range of the antiferroelectric phase. This is due to the ϑ^4 dependence of the ORP in tilted and chiral smectic phase. Because in this region, the tilt angle increases as $(T_c-T)^{0.25}$, the ORP grows linearly with temperature, $\rho\approx\vartheta^4\approx(T_c-T)$.

V. CONCLUSIONS

In this paper we have shown that high resolution birefringence data in tilted and chiral smectics can give valuable information on the structural properties and phase transitions between these phases. The method of measuring the birefringence is highly accurate and sensitive to any small change of the tilt angle and can reveal surprising details in the vicinity of phase transitions. In particular, we have clearly shown that in the smectic-A phase there are strong pretransitional fluctuations, characteristic for the materials, exhibiting the antiferroelectric phases, which tend to reduce the optical anisotropy. Further, we have shown that the smectic-A–smectic-C^*_α phase transition is continuous. However, the temperature dependence of the tilt angle as well as the theoretical analysis clearly indicate that this transition is close to the tricritical point. This means that six-order terms have to be included in the free-energy expansion for these materials. We have also shown that all the reconstructive phase transitions between the smectic-C^*_α, smectic-C^*, smectic-C^*_γ, and smectic-C^*_A phases are of first order and are accompanied by discontinuous jumps of the tilt angle. These experimental observations have been quantitatively explained within the framework of the discrete model of Čepič and Žekš [8,9], which includes next-nearest-neighbor interactions. We also present the first set of experimentally determined coefficients for this model. The good agreement between the theory and experiment clearly indicates the relevance of this model for the thermodynamics of tilted chiral smectics with antiferroelectric and intermediate phases. This good quantitative agreement is also an indirect indication that the structures of the smectic-C^*_α and smectic-C^*_γ phases, as shown in Figs. 1(c) and 1(d) could indeed be real. The final proof, however, still remains to be performed.

[1] C. Y. Young, R. Pindak, N. A. Clark, and R. B. Meyer, Phys. Rev. Lett. **40**, 773 (1978); S. Heinekamp, R. A. Pelcovits, E. Fontes, E. Yi Chen, R. Pindak, and R. B. Meyer, *ibid.* **52**, 1017 (1984); Y. Galerne and L. Liebert, *ibid.* **66**, 2891 (1991); Y. Galerne and L. Liebert, Phys. Rev. Lett. **64**, 906 (1990); Ch. Bahr and D. Fliegner, Phys. Rev. Lett. **70**, 1842 (1993).

[2] K. Hiraoka, Y. Takanishi, H. Takezoe, A. Fukuda, T. Isozaki, Y. Suzuki, and I. Kawamura, Jpn. J. Appl. Phys. **31**, 3394 (1992).

[3] E. Gorecka, A. D. L. Chandani, Y. Ouchi, H. Takezoe, and A. Fukuda, Jpn. J. Appl. Phys. **29**, 131 (1990); T. Isozaki, K. Hiraoka, Y. Takanishi, H. Takezoe, A. Fukuda, Y. Suzuki, and I. Kawamura, Liq. Cryst. **12**, 59 (1992); Ch. Bahr, D. Fliegner,

C. J. Booth, and J. W. Goodby, Phys. Rev. E **51**, R3823 (1995).
[4] J. Lee, A. D. L. Chandani, K. Itoh, Y. Ouchi, H. Takezoe, and A. Fukuda, Jpn. J. Appl. Phys., Part 1 **29**, 1122 (1990).
[5] H. Orihara and Y. Ishibashi, Jpn. J. Appl. Phys., Part 2 **29**, L115 (1990).
[6] B. Žekš, M. Čepič, Liq. Cryst. **14**, 445 (1993).
[7] M. Yamashita, J. Phys. Soc. Jpn. **65**, 2904 (1996).
[8] M. Čepič and B. Žekš, Mol. Cryst. Liq. Cryst. Sci. Technol., Sect. A **263**, 61 (1995).
[9] M. Čepič and B. Žekš (unpublished).
[10] V. L. Lorman, A. A. Bulbitch, and P. Toledano, Phys. Rev. E **49**, 1367 (1994); A. Roy and N. V. Madhasudana, Europhys. Lett. **36**, 221 (1996); H. Sun, H. Orihara, and I. Ishibashi, J. Phys. Soc. Jpn. **8**, 2706 (1993); S. A. Pikin, S. Hiller, and W. Haase, Mol. Cryst. Liq. Cryst. Sci. Technol., Sect. A **262**, 425 (1995).
[11] J. Philip, J. R. Lalanne, J. P. Marcerou, and G. Sigaud, Phys. Rev. E **52**, 1846 (1995); J. Philip, J. R. Lalanne, J. P. Marcerou, and G. Sigaud, J. Phys. II **4**, 2149 (1994).
[12] I. Muševič, M. Škarabot, R. Blinc, W. Schranz, and P. Dolinar, Liq. Cryst. **20**, 771 (1996).
[13] M. Čepič and B. Žekš, Liq. Cryst. **20**, 29 (1996).
[14] I. Muševič, Th. Rasing, B. Žekš, and R. Blinc, in *Liquid Crystals in the Nineties and Beyond* (World Scientific, Singapore, 1996).
[15] J. C. Kemp, J. Opt. Soc. Am. **59**, 950 (1969).
[16] K. C. Lim and J. T. Ho, Phys. Rev. Lett. **40**, 1576 (1978).
[17] C. C. Huang and J. M. Viner, Phys. Rev. A **25**, 3385 (1982).
[18] A. Seppen, I. Muševič, G. Maret, B. Žekš, P. Wyder, and R. Blinc, J. Phys. (France) **49**, 1569 (1988).
[19] P. Gisse, V. L. Lorman, J. Pavel, and H. T. Nguyen, Ferroelectrics **178**, 297 (1996).